Reduced G Protein-coupled Signaling Efficiency in Retinal Rod Outer Segments in Response to *n*-3 Fatty Acid Deficiency*

Shui-Lin Niu, Drake C. Mitchell, Sun-Young Lim, Zhi-Ming Wen, Hee-Yong Kim, Norman Salem, Jr., and Burton J. Litman‡

From the Laboratory of Membrane Biochemistry and Biophysics, National Institute on Alcohol Abuse and Alcoholism, Rockville, Maryland 20852

The fatty acid (FA) docosahexaenoic acid (DHA, 22:6*n*-3) is highly enriched in membrane phospholipids of the central nervous system and retina. Loss of DHA because of *n*-3 FA deficiency leads to suboptimal function in learning, memory, olfactory-based discrimination, spatial learning, and visual acuity. G protein-coupled receptor (GPCR) signal transduction is a common signaling motif in these neuronal pathways. Here we investigated the effect of *n*-3 FA deficiency on GPCR signaling in retinal rod outer segment (ROS) membranes isolated from rats raised on *n*-3-adequate or -deficient diets. ROS membranes of second generation *n*-3 FA-deficient rats had ~80% less DHA than *n*-3-adequate rats. DHA was replaced by docosapentaenoic acid (22:5*n*-6), an *n*-6 FA. This replacement correlated with desensitization of visual signaling in *n*-3 FA-deficient ROS, as evidenced by reduced rhodopsin activation, rhodopsin-transducin (G$_t$) coupling, cGMP phosphodiesterase activity, and slower formation of metarhodopsin II (MII) and the MII-G$_t$ complex relative to *n*-3 FA-adequate ROS. ROS membranes from *n*-3 FA-deficient rats exhibited a higher degree of phospholipid acyl chain order relative to *n*-3 FA-adequate rats. These findings reported here provide an explanation for the reduced amplitude and delayed response of the electroretinogram a-wave observed in *n*-3 FA deficiency in rodents and nonhuman primates. Because members of the GPCR family are widespread in signaling pathways in the nervous system, the effect of reduced GPCR signaling due to the loss of membrane DHA may serve as an explanation for the suboptimal neural signaling observed in *n*-3 FA deficiency.

G protein-coupled receptor (GPCR)[1] signaling is ubiquitous in the retina, brain, and nervous system and includes vision, taste, odor, and many neurotransmitter and channel signaling pathways leading to cognitive function (1). Docosahexaenoic

acid (DHA, 22:6*n*-3), a long chain polyunsaturated fatty acid (FA) of the *n*-3 series, is highly enriched in the membrane phospholipids of the brain, neuronal tissue, and retina (2). In *n*-3 FA deficiency, membrane phospholipid DHA is replaced in both the retina and brain by docosapentaenoic acid (DPA, 22:5*n*-6), an *n*-6 series FA, in a near stoichiometric manner (3). *n*-3 deficiency is associated with visual and cognitive deficits, as observed in animal and human infant studies (2). Studies in reconstituted systems demonstrate that visual signaling, the best characterized GPCR system, is sensitive to membrane phospholipid acyl chain composition and appears to be optimal in DHA membranes (4). An important question in determining the underlying mechanism responsible for the deficits observed in *n*-3 FA deficiency is whether the loss of DHA *in vivo* results in suboptimal GPCR signaling.

In visual signaling, absorption of a photon by rhodopsin triggers the formation of the active form of the receptor, metarhodopsin II (MII) (5). MII binds and activates several hundred molecules of transducin (G$_t$), the visual G protein (6), which subsequently activates the effector enzyme, a cGMP phosphodiesterase (PDE). PDE catalyzes cGMP hydrolysis, triggering closure of cGMP-gated Na$^+$/Ca^{2+} channels in the rod outer segment (ROS) plasma membrane. This hyperpolarizes the rod cell and initiates the visual response, as observed in the a-wave of the electroretinogram (ERG). Thus, the ERG a-wave time course and amplitude are determined by the kinetics and coupling parameters of the individual steps in the visual signaling pathway. Early studies of the FA dependence of the ERG showed that decreased levels of *n*-3 FAs in the diet led to decreased a-wave and b-wave amplitudes in the rat ERG (7). Similar changes were observed in the ERGs of rodents (8, 9) and cats (10). *n*-3 FA deficiency was also associated with increased implicit times in the ERG and decreased visual acuity in nonhuman primates (11–13). The most dramatic change observed in the composition of the retinal tissue is the replacement of DHA by DPA, suggesting that depletion of retinal DHA is responsible for the observed suboptimal responses, likely through changes in membrane physical properties that lead to down-regulation of GPCR signaling pathways.

In this study, we provide explicit experimental evidence linking the changes in phospholipid acyl chain composition associated with *n*-3 FA deficiency to the down-regulation of individual steps in a GPCR signaling pathway using the visual signaling pathway as a model system. The replacement of DHA by DPA in *n*-3 FA-deficient rat ROS resulted in slower kinetics and reduced levels of receptor activation, receptor-G protein coupling, and an attenuation of the integrated signaling pathway, as evidenced by a 3-fold reduction in PDE activity at physiologically relevant bleach levels. In addition, ROS membranes from *n*-3-deficient rats had a higher degree of phospho-

---

[1] The abbreviations used are: GPCR, G protein-coupled receptor; DHA or 22:6*n*-3, docosahexaenoic acid; DPA or 22:5*n*-6, docosapentaenoic acid; FA, fatty acid; MI and MII, metarhodopsin I and II, respectively; G$_t$, transducin; PDE, phosphodiesterase; ROS, rod outer segment(s); ERG, electroretinogram; HPLC, high pressure liquid chromatography; DPH, diphenylhexatriene; PE, phosphatidylethanolamine; PC, phosphatidylcholine; PS, phosphatidylserine; PLE, plasmalogen PE; TBS, Tris-buffered saline; DTPA, diethylenetriaminepentaacetic acid.

lipid acyl chain order than those obtained from *n*-3-adequate rats. These studies provide a mechanistic basis for the reduced amplitude and delayed response (increased latency) of the retinal ERG a-wave observed in *n*-3 FA-deficient animals.

MATERIALS AND METHODS

Animal Procedures—The protocol and all animal procedures used in this experiment were approved by the Animal Care and Use Committee of the National Institute on Alcohol Abuse and Alcoholism. Female Long-Evans rats were obtained from Charles River (Portage, MI) at weaning (3 weeks of age). Weaning females were semirandomly divided into two dietary groups with the constraint that both groups had the same mean body weight. One group of females was fed with the *n*-3 FA-adequate diet, and the second group was fed with the *n*-3 FA-deficient diet (14). The females in both dietary groups were mated with 12-week-old males when they were 11 weeks of age. Offspring were culled to a maximum of 12/dam, and the dams were maintained on their respective diets during lactation. At the age of 21 days, the pups were dark-adapted overnight and sacrificed by decapitation under dim red light.

Diet Composition—Diets were patterned after those of the American Institute of Nutrition (AIN93) with the fat source modified to provide either a low or an adequate level of *n*-3 FAs. Both diets had the same basal macronutrients, vitamins, minerals, and basal fats (hydrogenated coconut and safflower oils) (14). However, the *n*-3 FA-adequate diet also contained flaxseed oil and DHASCO® (Martek Biosciences, Columbia, MD), fats that supply α-linolenic acid and DHA, respectively, as their principal component. FA composition of the diets was balanced for saturated FAs, monounsaturated FAs, and linoleic acid; the key difference between diets was a substitution of a small amount of flaxseed and DHASCO® oils for a portion of the hydrogenated coconut oil in the *n*-3 FA-adequate diet.

ROS Membrane Sample Preparation—Retinas were dissected immediately after sacrifice under dim red light and placed in 10 ml of TBS (10 mM Tris, 60 mM KCl, 30 mM NaCl, 2 mM MgCl$_2$, 50 μM DTPA, 2 mM dithiothreitol, and 15 μg of aprotinin, pH 8.0) at 4 °C. ROS were prepared using a sucrose gradient method as described previously (15). The endogenous peripheral membrane proteins, G$_t$ and PDE, in ROS were removed by two washes in hypotonic buffer (5 mM Tris and 50 μM DTPA, pH 8.0). The purified ROS membranes were assayed for rhodopsin contents and the concentration of total phospholipids. Aliquots of G$_t$ and PDE isolated from bovine retinas were added back to the hypotonically stripped ROS membranes at the physiological ratio of 100:10:1 of rhodopsin:G$_t$:PDE to restore the signaling cascade (16).

Phospholipid Analysis—Phospholipid molecular species were analyzed using reversed phase HPLC-electrospray mass spectrometry (17). Lipids were extracted from ROS membranes using the Bligh and Dyer procedure in the presence of deuterium-labeled phospholipid internal standards. Samples were injected into a C$_{18}$ column and separated using a mobile phase containing 0.5% NH$_4$OH in water, methanol, and hexane and a gradient from 12:88:0 to 0:88:12 in 17 min at a flow rate of 0.4 ml/min after holding at the initial composition for 3 min. The separated phospholipid molecular species were detected using an Agilent HPLC-MS 1100 Series mass selective detector instrument. For electrospray ionization the capillary voltage and the exit voltage were set at 4000 and 200 V, respectively. The drying gas temperature was set at 350 °C, the flow rate of the drying gas was 13 liters/min, and the gas pressure of the nebulizer was 32 p.s.i. Quantification was based on the area ratios calculated against the internal standard of the same phospholipid class.

Assays—Light-activated PDE activity was assayed using a real time pH method (18) with the following modifications. A high sensitivity pH meter with built-in temperature compensation (Model 370 from Thermo Orion, Beverly, MA) coupled to a microelectrode (MI-710 from Microelectrodes, Inc., Bedford, NH) was used to monitor pH. The signal output from the pH meter was acquired by a computer through a 12-bit A/D board (Lab-PC-1200/AI, National Instruments, Austin, TX) operated at a 1-kHz rate. Samples that contained 5 μM rhodopsin from either *n*-3 FA-adequate or -deficient ROS membranes with replenished bovine G$_t$ and PDE, 50 μM GTP, and 1 mM cGMP in TBS buffer (pH 8.0) were preincubated at 37 °C in a thermo-regulated microcuvette in the dark for 10 min. A set of 20 data points was collected as the base-line activity prior to sample activation by a flash lamp (FX1131 from EG&G; pulse width = 1 μs) synchronized by the computer. The light intensity was attenuated using neutral density filters to vary the level of rhodopsin activation in samples, which was determined by rhodopsin concentrations before and after light exposure. The PDE activity is ob-

tained from the shift in pH and is expressed as cGMP hydrolyzed (mM)/s. Rhodopsin activation was characterized by the MI-MII equilibrium constant, K_{eq}, using a spectroscopic method (19, 20).

Time-resolved Fluorescence Measurements—Fluorescence lifetime and differential polarization measurements were performed with a K2 multifrequency cross-correlation phase fluorometer (ISS, Urbana, IL) as described previously (21). For lifetime measurements 12 modulation frequencies were used, logarithmically spaced from 5 to 200 MHz, and differential polarization measurements were made at 15 modulation frequencies logarithmically spaced from 5 to 200 MHz. Both total intensity decay and differential polarization measurements were repeated a minimum of three times. Measured polarization-dependent differential phases and modulation ratios for each sample were combined with the measured total intensity decay to yield the anisotropy decay, $r(t)$. Anisotropy decay data of diphenylhexatriene (DPH) were analyzed using the Brownian rotational diffusion model (21). This model characterizes the anisotropy decay of DPH in terms of the orientational distribution function, $f(\theta)$, and the diffusion coefficient for rotation about the long axis of DPH.

Flash Photolysis Measurements—Samples for flash photolysis measurements were prepared by diluting concentrated ROS suspensions with pH 7.5 TBS buffer, dividing the solution in half, and adding concentrated G$_t$ to one half and an identical amount of G$_t$ buffer to the other half. Samples were then incubated for 4 h on ice to ensure binding of G$_t$ to the bilayer. Final concentrations were 5.0 μM rhodopsin and 1.0 μM G$_t$. Kinetics of MII and MII-G$_t$ formation were assessed by measuring the transient absorption at 380 nm using a flash photolysis system as described previously (22). Excitation was provided by a high pressure flash lamp (EG&G; pulse width = 1 μs) filtered with a broad ($\pm$25 nm) bandpass filter centered at 500 nm. The current from a thermoelectrically cooled photomultiplier tube (R928, Hamamatsu) was passed to a low noise current amplifier (Stanford Research). The amplifier output voltage was acquired at 2–10 μs/point by a 1.25-MHz, 12-bit analog-to-digital converter (National Instruments) installed in a personal computer.

The detailed kinetics of MII formation were extracted from the changes in absorbance observed at 380 nm in the absence of G$_t$ via analysis in terms of the microscopic rate constants of a branched photoreaction model (19). The kinetics of MII-G$_t$ formation were determined by analyzing absorbance changes at 380 nm obtained in the presence of G$_t$ in terms of the branched model plus a reaction between MII and G$_t$ to form the MII-G$_t$ complex. In both cases the observed absorbance increase at 380 nm was directly analyzed in terms of the appropriate microscopic rate constants using NONLIN with subroutines specifying each model written by the authors of this paper.

Flash photolysis measurements in the presence of G$_t$ produced an equilibrium mixture of MI, free MII, and MII-G$_t$ complex. MI and free MII were assumed to be present in the ratio corresponding to their equilibrium mixture measured in the absence of G$_t$, and the concentrations of free MII and MII-G$_t$ complex were determined from the kinetic analysis. The association constant, K_a, between MII and G$_t$ was determined using the measured concentrations of free MII and MII-G$_t$ complex and assuming that [free G$_t$] = [total G$_t$] − [MII-G$_t$ complex].

RESULTS

Lipid and Protein Analysis—To characterize the effect of the dietary regimes on ROS membrane lipid composition, phospholipid molecular species and total acyl chain composition for each phospholipid class were determined for both *n*-3 FA-adequate and -deficient dietary groups. The *n*-3 FA-adequate group contained the highest levels of DHA in phosphatidylserine (PS) and phosphatidylethanolamine (PE) at 44.7 ($\pm$0.9)% and 49.8 ($\pm$0.4)% of total acyl chains, respectively. DHA levels in phosphatidylcholine (PC) and plasmalogen PE (PLE) were lower at 29.4 ($\pm$0.9)% and 24.5 ($\pm$0.4)%, respectively (Table I). Only minor levels of DPA were detected in all classes analyzed. Relative to the *n*-3 FA-adequate diet, the *n*-3 FA-deficient diet resulted in a major loss of DHA in PC, PS, PE, and PLE of 79, 79, 73, and 82%, respectively. The reduction in DHA was accompanied by a compensatory replacement by the *n*-6 FA, DPA, a close structural analog of DHA with one less double bond at the *n*-3 position. This is consistent with the essentially reciprocal replacement of DHA by DPA associated with *n*-3 FA deficiency that was observed by others (3). Differ-

DHA and Signal Transduction

TABLE I

Phospholipid compositions of ROS membranes

ROS membranes were obtained from 3-week-old second generation rats raised on either an *n*-3 FA-adequate or -deficient diet.

Lipid class	*n*-3 adequate		*n*-3 deficient	
	22:6*n*-3[a]	22:5*n*-6[a]	22:6*n*-3[a]	22:5*n*-6[a]
	%		%	
PC	29.4 ($\pm$ 0.9)	0.8 ($\pm$ 0.0)	6.2 ($\pm$ 0.1)	22.2 ($\pm$ 0.2)
PS	44.7 ($\pm$ 0.9)	2.4 ($\pm$ 0.2)	9.4 ($\pm$ 0.8)	36.2 ($\pm$ 0.2)
PE	49.8 ($\pm$ 0.4)	1.8 ($\pm$ 0.1)	13.5 ($\pm$ 0.1)	31.3 ($\pm$ 0.4)
PLE	24.5 ($\pm$ 0.4)	1.8 ($\pm$ 0.1)	4.5 ($\pm$ 0.2)	15.0 ($\pm$ 0.4)

[a] Percentages of 22:6*n*-3 or 22:5*n*-6 are expressed as the mole percentage of total fatty acid in each phospholipid class. Values in parentheses are S.D.

ences for key phospholipid molecular species are illustrated in Fig. 1. DHA is the major phospholipid component in the *n*-3 FA-adequate ROS. A significant amount of PC, PS, and PE contains DHA in both the *sn*-1 and *sn*-2 acyl chain positions. In contrast, ROS from *n*-3 FA-deficient rats show a major loss of DHA, which is accompanied by the appearance of DPA-containing species as the primary constituents. One of the interesting findings is that the di-22:6*n*-3 species of PE and PC are not well replaced by di-22:5*n*-6 species; instead, there is an increased level of 18:0,22:5*n*-6 PC in the ROS from *n*-3 FA-deficient rats. There is also a failure in the replacement of 16:0,22:6*n*-3 PLE species by the corresponding DPA species. The ratio of membrane phospholipid to rhodopsin was determined to be the same for both dietary groups, suggesting that rhodopsin expression was not altered by *n*-3 FA deficiency.

Light-stimulated PDE Activity—The PDE activity, which is a measure of the integrated activity of the visual signaling pathway encompassing rhodopsin activation, MII-G_t coupling, $G_{t\alpha}$-PDE coupling, and PDE-catalyzed cGMP hydrolysis, was assayed for ROS membranes isolated from *n*-3 FA-adequate and -deficient rat retinas. ROS membranes were hypotonically stripped of endogenous G_t and PDE and subsequently reconstituted with equivalent aliquots of the same preparation of purified bovine G_t and PDE so as to restore the native ratio of proteins in the visual pathway. This was done to ensure that *n*-3 FA-adequate and -deficient ROS membranes contained identical amounts of G_t and PDE so that the only difference in the two samples was the change in ROS membrane phospholipid composition induced by the diet. Thus any changes observed in light-stimulated PDE activity can unequivocally be associated with the observed changes in ROS membrane composition.

The ROS membranes from both dietary groups exhibited similar dark PDE activity, as shown from the base line in the absence of light stimulus (Fig. 2*a*). Upon light stimulation, which activates a fraction of 1.7×10^{-3} rhodopsin molecules, there were considerable differences in the amplitude and the rate of cGMP hydrolysis observed for ROS membranes derived from *n*-3 FA-adequate and -deficient rat retinas. These differences were dependent on the level of light stimulus, which is shown in the dose-response curve (Fig. 2*b*), where the PDE activity is expressed as a percentage of the maximal rate of cGMP hydrolysis and the light stimulus level is expressed as the fraction of rhodopsin molecules light-activated. The dose-response curve is shifted toward the right for the *n*-3 FA-deficient group, indicating a loss of sensitivity of the light-activated signaling pathway (Fig. 2*b*). High levels of light stimulus saturated the light-activated PDE activity and diminished the difference in PDE activity between the two dietary groups. However, the large difference in PDE activity in the ROS samples at low light stimulus levels is explicitly shown in the plot of the ratio of PDE activity in *n*-3 FA-adequate ROS to that in *n*-3 FA-deficient ROS (Fig. 2*c*). Under physiological conditions, where about 1 in 10^5 rhodop-

sin molecules is activated, there was a ~3-fold difference between light-stimulated PDE activity in *n*-3 FA-adequate ROS and *n*-3 FA-deficient ROS.

Receptor Activation—To identify the steps involved in the change in visual pathway sensitivity induced by *n*-3 FA deficiency, we measured the level and rate of rhodopsin activation in ROS membranes from both dietary groups. The MI-MII equilibrium constant, $K_{eq} = [MII]/[MI]$, which is a measure of the level of rhodopsin activation, was reduced by 16% at 37 °C in ROS membranes from the *n*-3 FA-deficient group relative to the *n*-3-adequate group (Fig. 3*a*). This observation in the ROS membrane is consistent with the lower K_{eq} values observed previously for rhodopsin reconstituted in membranes containing phospholipids with lower DHA or acyl chain unsaturation levels (20). The time constant for MII formation at 37 °C, τ_{MII}, in the *n*-3 FA-adequate group was 0.56 ms, compared with 0.67 ms in the deficient group (Fig. 3*b*). This translates into ~20% delay in the rate of MII formation induced by *n*-3 FA deficiency. Previous studies established that DHA-containing membranes have relatively low membrane acyl chain order parameters (23), high compressibility (24), and high membrane acyl chain packing free volume (21). Given that a molecular volume expansion is associated with the MI to MII transition, the properties of DHA membranes would likely impose a minimal energy barrier for the formation of MII, whereas a reduction in DHA levels in *n*-3 FA-deficient ROS membranes would likely raise the energy barrier. This is consistent with the reduced acyl chain packing free volume observed for the ROS membranes from the *n*-3 FA-deficient group relative to the *n*-3-adequate group (see "Membrane Structure" below). This variation in membrane properties would affect both the extent and the rate of formation of MII.

Receptor-G Protein Coupling—The initial step in signal amplification and information flow from receptor to effector enzyme in GPCR signaling is the formation of an activated receptor-G protein complex, which is the MII-G_t complex in the visual system. The association constant, K_a, for the complex is 16.4 μM^{-1} for the *n*-3-adequate ROS and 9.9 μM^{-1} for the *n*-3-deficient ROS. This demonstrates that lower levels of the MII-G_t complex form in the *n*-3 FA-deficient ROS. In the *n*-3 FA-adequate group, the time constant for MII-G_t formation, τ_{MII-Gt}, is 0.81 ms, paralleling closely the kinetics of MII formation, which has a time constant of 0.56 ms. The tight coupling of MII appearance and MII-G protein complex formation makes visual transduction one of the most efficiently coupled systems in the GPCR family. However, in the *n*-3 FA-deficient ROS, the kinetics of MII-G_t formation were slower than those of the adequate group by 38% (Fig. 3*c*). The ratio of the time constants $\tau_{MII-Gt}:\tau_{MII}$ is a measure of the lag time in the coupling of MII to G_t. This ratio is 1.45 for the *n*-3 FA-adequate ROS and is increased by 16% to 1.67 in the *n*-3 FA-deficient ROS, indicating a reduced efficiency of MII coupling to G_t. The overall lag time in the initiation of the ERG a-wave is determined by the fact that the time constant for the appearance of

FIG. 1. **Molecular species analysis of various phospholipid classes in *n*-3 fatty acid-adequate (*open bars*) and -deficient (*hatched bars*) ROS membranes.**
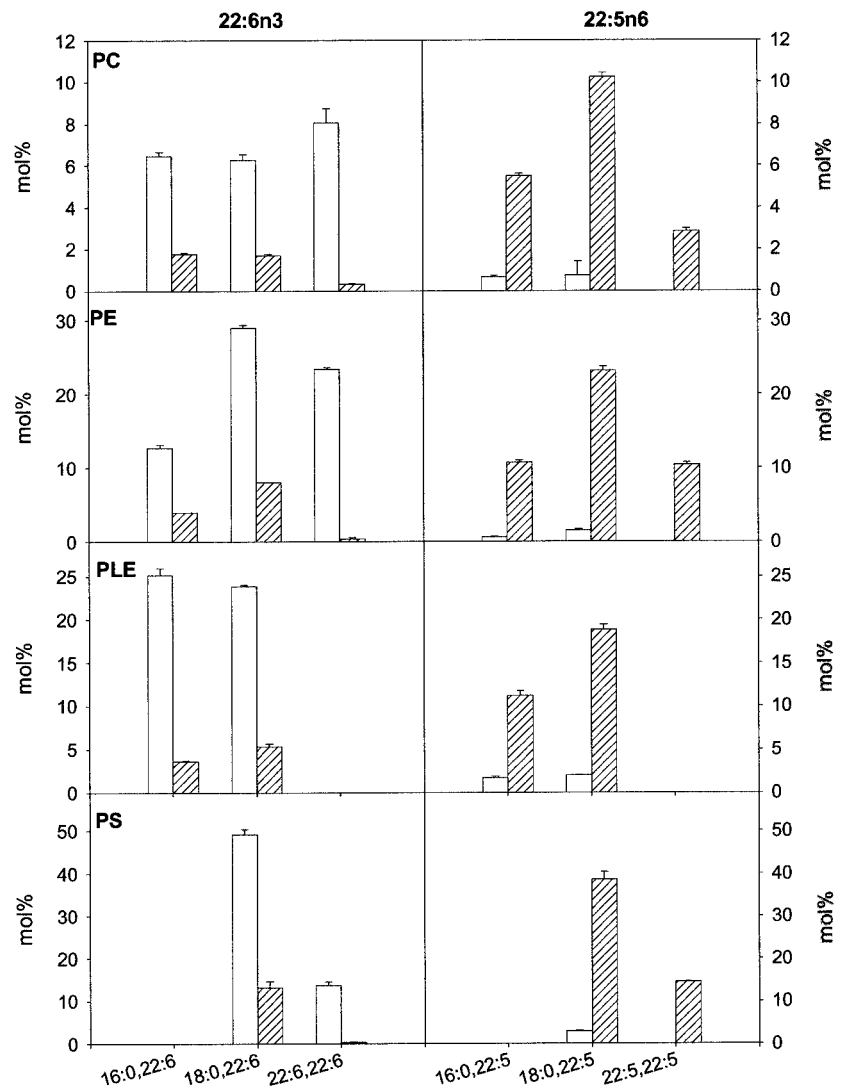
the MII-G_t complex is 38% larger in the *n*-3-deficient ROS than in the *n*-3-adequate ROS. A previous study, using reconstituted membranes, demonstrated that the rate of MII-G_t formation, which is controlled by lateral diffusion of MII and G_t in the plane of the membrane, is mediated by phospholipid acyl chain composition and optimized in DHA-containing bilayers (22). A similar dependence would explain the observed delay in the formation of MII-G_t in the *n*-3 FA-deficient ROS membranes.

Membrane Structure—Time-resolved fluorescence anisotropy of the hydrophobic fluorescent probe DPH was shown to be a reliable probe of acyl chain packing properties in both reconstituted rhodopsin-lipid vesicles and ROS disk membranes (22, 25). Analyzing the data using a Brownian rotational diffusion model yields a parameter f_v, which allows a comparison of relative acyl chain packing free volume in membranes of different lipid composition. This parameter decreases with increasing acyl chain order. Values of f_v for ROS membranes from *n*-3 FA-adequate and -deficient rats are 0.11 and 0.086, respectively. The smaller f_v value for the *n*-3 FA-deficient ROS membranes indicates a more ordered phospholipid acyl chain packing than that of the *n*-3 FA-adequate ROS membranes.

DISCUSSION

ERGs of *n*-3 FA-deficient rodents and nonhuman primates are characterized by a reduced amplitude and increased latency in the a-wave, which is determined by the visual transduction pathway in the ROS. The rate and degree of hyperpo-

larization of the ROS plasma membrane, which results from the closure of cGMP-gated Na^+/Ca^{2+} channels, are determined by the rate and extent of hydrolysis of cGMP by the PDE. Characteristics of the light-stimulated PDE activity in turn depend on the rate and extent of rhodopsin activation to MII, MII activation of G_t, and the resulting activation of the PDE by $G_{t\alpha}$. A recently published model relates the generation of the ERG a-wave to the kinetic and equilibrium parameters associated with the various steps in the visual transduction pathway (26). The model explicitly relates the amplitude of the ERG a-wave to the number of activated rhodopsin molecules and the subsequent number of G proteins and PDE catalytic subunits activated, whereas the rate of generation of the a-wave is associated with the kinetics of coupling of these proteins in the signaling pathway.
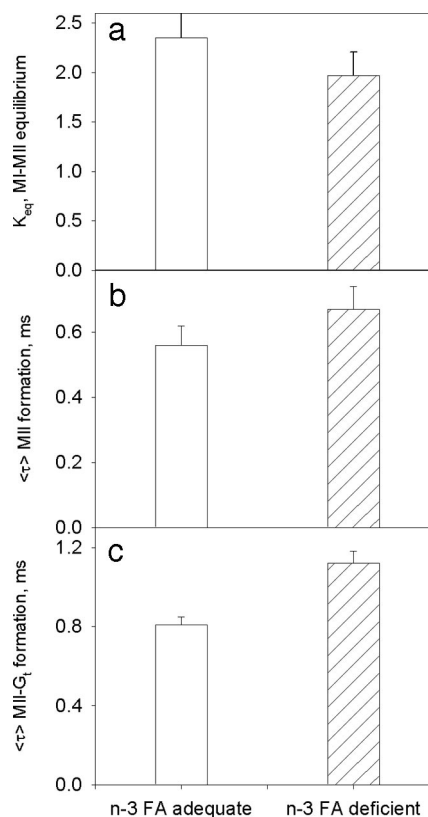
In the current study, we provide insight into the factors responsible for the observed changes in the ERG in *n*-3 deficiency by relating the changes in membrane physical properties, resulting from the replacement of DHA by DPA, to functional differences observed in the visual signaling pathway. The visual pathway is triggered by the light-stimulated activation of the visual receptor, rhodopsin, to form MII. The first step in signal amplification is formation of the receptor-G protein complex (MII-G_t). The level of PDE activity is a direct consequence of the level of rhodopsin activation and the efficiency of the subsequent activation steps leading to PDE acti-
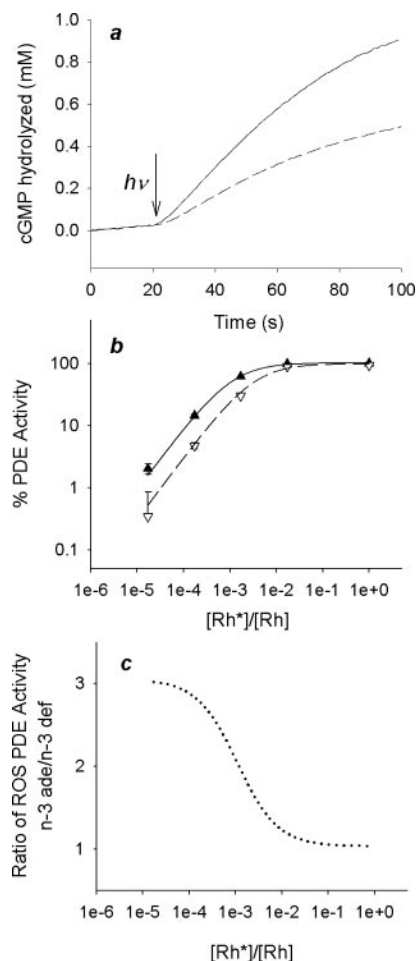
FIG. 2. **Light-stimulated PDE activity in ROS from *n*-3 fatty acid-adequate and -deficient rats.** *a*, example of a time course of PDE-catalyzed cGMP hydrolysis at a rhodopsin activation level of 0.17% in the *n*-3 fatty acid-adequate group (*solid line*) and the *n*-3 fatty acid-deficient group (*dashed line*). The *arrow* indicates the time point of the applied flash. *b*, dose-response curve for PDE activity at various levels of light stimulus in *n*-3-adequate (▲) and *n*-3 fatty acid-deficient (▽) ROS. The percentage of ROS PDE activity was normalized to that of the *n*-3 fatty acid-adequate group at maximum activation. Each *data point* was averaged from at least two independent measurements. *c*, comparison of ROS PDE activities from the two dietary groups at various levels of light stimulus. The plot was calculated as the ratio of PDE activity in the *n*-3 fatty acid-adequate group (*n*-3 ade) to that of the *n*-3-deficient group (*n*-3 def) from the fitted curves in Fig. 1*b*. [Rh*]/[Rh] is the fraction of rhodopsin that is activated by light and varies from 10^{-5} to 1 in these experiments.

FIG. 3. **Effect of *n*-3 fatty acid deficiency.** *a*, K_{eq} = [MII]/[MI], the MI-MII equilibrium constant. *b*, kinetics of MII formation, which is shown as the average time constant for MII formation. *c*, kinetics of MII-G_t formation, shown as the average time constant of MII-G_t formation. The *n*-3 fatty acid-adequate group is represented by the *open bar*, and the *n*-3 fatty acid-deficient group is represented by the *hatched bar*.

vation. At saturating levels of light stimulus, activated rhodopsin molecules are produced in large excess relative to G_t, resulting in saturation of visual signaling. This minimizes the differences in rhodopsin activation and MII-G_t formation produced by *n*-3 FA deficiency (Fig. 2, *b* and *c*). However, under typical physiological conditions, rhodopsin is activated at the level of about 1 in 10^5 molecules, yielding a MII to G_t ratio of about 1:10,000. This makes rhodopsin activation and MII-G_t formation rate-determining steps. Measurements at this stimulus level allow a better estimate of the physiological consequences of *n*-3 FA deficiency on the visual transduction pathway (Fig. 2, *b* and *c*). Here a 3-fold reduction in PDE activity is observed in the *n*-3 FA-deficient ROS relative to the *n*-3-adequate ROS in response to identical light stimuli.

We observed a difference in the MI-MII equilibrium constant, K_{eq}, of about 16%, which will lead to a reduction of about 12% in the number of rhodopsin molecules reaching the activated MII state. In addition, values of K_a, the association

constant for the formation of the MII-G_t complex, of 16.4 and 9.9 μM^{-1} were determined in the *n*-3-adequate and -deficient samples, respectively. This represents a 66% drop in K_a, which coupled with a lower level of MII formation results in a 23% lower concentration of MII-G_t formed in the deficient ROS relative to the adequate ROS. Complex formation represents the initial amplification step in the visual pathway and is required for G_t activation. If the activation process is similarly affected, then there will be a ~23% loss in activated G_t molecules. The reduced level of activated G_t will translate into lower levels of PDE activation. The observed reduction in ROS PDE activity in the *n*-3 FA-deficient group will result in a reduced level of rod plasma membrane hyperpolarization, resulting in a reduced response, as measured by the ERG a-wave. This is consistent with the reduced amplitude in the retinal ERG a-wave observed in various *n*-3 FA-deficient rodent and non-human primate studies (7, 8, 10, 27).

The time constant τ_{MII-Gt} for MII-G_t complex formation, which is a measure of the coupling of the activated receptor to the G protein, is dependent on lateral diffusion of the receptor and G protein in the plane of the disk membrane. The value of τ_{MII-Gt} in ROS from *n*-3 FA-adequate rats is 0.81 ms, and the value of τ_{MII-Gt} in ROS from the *n*-3 FA-deficient group is 1.12 ms. This represents a 0.31-ms delay in receptor-G protein coupling, which will manifest as an increased latency in signal development in the pathway. The additional coupling step in the signaling pathway between $G_{t\alpha}$ and PDE is also dependent on membrane lateral diffusion. Therefore, it is likely to be affected by membrane DHA levels in a manner similar to the MII-G_t step and would further contribute to latency in PDE activation and subsequent generation

of neuronal signaling, as measured by the ERG a-wave, in the retinas of *n*-3 FA-deficient rats.

Our data for the first time provides direct evidence that an *n*-3 FA-deficient diet reduces the efficiency of individual steps in a GPCR signaling pathway. The only difference between the ROS samples from *n*-3 FA-adequate and -deficient rats was the FA composition of the membranes. *n*-3 FA deficiency was associated with about an 80% loss of DHA in ROS membranes with compensatory replacement of DHA by DPA. Otherwise, samples were matched for content of rhodopsin, G protein, PDE, and light stimulus in various experiments. Remarkably, the difference in phospholipid acyl chain content of the ROS membranes induced by *n*-3 FA deficiency resulted in lower levels of rhodopsin activation, reduced and delayed rhodopsin-G_t coupling, and reduced activity in the integrated signaling pathway, as measured by the PDE dose-response data. The replacement of DHA by DPA is a characteristic observation in the retina and brain of *n*-3 FA-deficient animals (2). The increased accretion of this unusual FA in the retina and brain highlights the functional requirement for phospholipids containing highly unsaturated acyl chains and DHA in particular. The exquisite sensitivity and fine tuning of the membrane properties in these tissues are evidenced by the fact that the loss of a single double bond at the *n*-3 position of DHA, corresponding to the structure of DPA, is enough to induce functional deficits in retinal signaling pathways. The observations in this study are supported by findings in previous reconstitution experiments, which have demonstrated the efficacy of DHA-containing phospholipids to enhance various steps in visual signaling (20, 22).

An explanation of the functional changes observed as a result of substitution of DPA for DHA in ROS phospholipids likely lies in the subtle changes in physical properties associated with the exchange of acyl chains. Previous studies in both native ROS disks and reconstituted bilayer systems demonstrated a direct link between phospholipid acyl chain packing properties, the level and kinetics of MII formation, and the level and kinetics of formation of MII-G_t (20, 22). The conformation change associated with MII formation involves an increase in molecular volume, which is energetically less favored in bilayers in which phospholipid acyl chains are more ordered, resulting in lower levels of MII formed. The interaction between MII and G_t requires a diffusional search process within the plane of the disk. Here again, a more highly ordered bilayer will result in slower diffusion rates and increase the time constant for MII-G_t complex formation. This same consideration applies to the activation of the PDE by G_t because this interaction also requires a diffusional search process within the plane of the disk membrane, which would further delay the activation of the PDE. Differences in acyl chain packing between membranes containing DHA and DPA phospholipids have been demonstrated by several physical techniques. NMR demonstrates that the DHA-containing phospholipids are more flexible at the methyl end of the chain and undergo more rapid conformational changes than DPA-containing phospholipids (28). Time-resolved fluorescence measurements on the ROS membrane preparations used in the current experiments also show a higher degree of acyl chain order in the *n*-3 FA-deficient, DPA-containing ROS membranes relative to the *n*-3 FA-adequate, DHA-containing ROS membranes. Changes in the functional properties of the visual transduction pathway, seen in previous studies in both native disk and reconstituted membranes, resulting from changes in membrane physical properties are consistent with the differences observed in this study between DPA- and DHA-containing ROS membranes.

Although we have not been able to evaluate directly the effect of the differences in ROS membrane composition on the rate or extent of the interaction of activated G_t with PDE or its effect on PDE activation, it is clear from the parameters measured that the apparently subtle difference in structure, *i.e.* the loss of a double bond associated with the replacement of DHA by DPA, has a marked effect on both the unimolecular conformation change associated with receptor activation and the efficiency of the diffusion-dependent receptor-G protein coupling. Thus it is likely that the interaction of $G_{t\alpha}$ and the PDE and the activation of the PDE catalytic subunit are effected by the loss of DHA in the *n*-3 FA-deficient ROS membranes. The only difference in the *n*-3 FA-deficient and -adequate ROS membranes in our experiments is the replacement of DHA by DPA. The collective changes in both the level and rate of interaction of the proteins in the visual pathway resulting from the replacement of DHA by DPA appear to be sufficient to explain the reduced PDE activity in *n*-3 FA-deficient ROS.

The current results and those from reconstitution experiments lead us to propose that the molecular mechanism responsible for the well documented deficits in visual physiology associated with *n*-3 FA-deficient diets (7, 29–32) is due in great part to the reduction in DHA in ROS membrane phospholipids. The reduced levels and longer times required for receptor activation and receptor-G protein coupling because of *n*-3 FA deficiency provide an explanation for the latency and reduced amplitude observed in the ERG a-wave of *n*-3 FA-deficient animals.

Many studies demonstrate that brain function is also compromised by the loss of DHA (1, 2). Poorer performance was observed in animal studies on such tasks as the Y-maze (33), active avoidance (34), brightness discrimination (35), shock avoidance (36), spatial tasks (14, 37, 38), olfaction-cued discrimination (39, 40), and neuromotor skills (41) when *n*-3-deficient diets are fed. Human infants perform more poorly on neurodevelopmental tests when given formulas without DHA relative to formulas with DHA (42–44). Considering the large number of neurotransmitter systems that utilize the GPCR signaling motif, the observed effect of the loss of DHA on visual signaling may well be generalized to GPCR signaling systems in the brain and provide an explanation of the suboptimal neuronal functions associated with *n*-3 FA deficiency. Thus, when the diet does not support adequate DHA accretion, alteration in GPCR function in the brain may result in suboptimal nervous system development and function.

REFERENCES

1. Salem, N., Jr., Litman, B., Kim, H. Y., and Gawrisch, K. (2001) *Lipids* **36,** 945–959
2. Salem, N. (1989) in *Current Topics in Nutrition and Disease: New Protective Roles for Selected Nutrients* (Spiller, G. A., and Scala, J., eds) pp. 109–228, Alan R. Liss Inc., New York
3. Galli, C., Trzeciak, H. I., and Paoletti, R. (1971) *Biochim. Biophys. Acta* **248,** 449–454
4. Litman, B. J., Niu, S. L., Polozova, A., and Mitchell, D. C. (2001) *J. Mol. Neurosci.* **16,** 237–242
5. Matthews, R. G., Hubbard, R., Brown, P. K., and Wald, G. (1963) *J. Gen. Physiol.* **47,** 215–240
6. Kibelbek, J., Mitchell, D. C., Beach, J. M., and Litman, B. J. (1991) *Biochemistry* **30,** 6761–6768
7. Wheeler, T. G., Benolken, R. M., and Anderson, R. E. (1975) *Science* **188,** 1312–1314
8. Weisinger, H. S., Vingrys, A. J., and Sinclair, A. J. (1996) *Ann. Nutr. Metab.* **40,** 91–98
9. Weisinger, H. S., Armitage, J. A., Jeffrey, B. G., Mitchell, D. C., Moriguchi, T., Sinclair, A. J., Weisinger, R. S., and Salem, N., Jr. (2002) *Lipids* **37,** 759–765
10. Pawlosky, R. J., Denkins, Y., Ward, G., and Salem, N., Jr. (1997) *Am. J. Clin. Nutr.* **65,** 465–472
11. Connor, W. E., and Neuringer, M. (1988) in *Biological Membranes: Aberrations in Membrane and Function Structure* (Karnosky, M. L., Lent, A., and Bolls, L. C., eds) pp. 275–276, Alan R. Liss Inc., New York
12. Neuringer, M., Connor, W. E., Lin, D. S., Barstad, L., and Luck, S. (1986) *Proc. Natl. Acad. Sci. U. S. A.* **83,** 4021–4025
13. Jeffrey, B. G., Mitchell, D. C., Hibbeln, J. R., Gibson, R. A., Chedester, A. L., and Salem, N., Jr. (2002) *Lipids* **37,** 839–848

14. Moriguchi, T., Greiner, R. S., and Salem, N., Jr. (2000) *J. Neurochem.* **75,** 2563–2573
15. Organisciak, D. T., Wang, H., and Kou, A. L. (1982) *Exp. Eye Res.* **34,** 401–412
16. Miller, J. L., Litman, B. J., and Dratz, E. A. (1987) *Biochim. Biophys. Acta* **898,** 81–89
17. Kim, H. Y., Wang, T. C., and Ma, Y. C. (1994) *Anal. Chem.* **66,** 3977–3982
18. Yee, R., and Liebman, P. A. (1978) *J. Biol. Chem.* **253,** 8902–8909
19. Straume, M., Mitchell, D. C., Miller, J. L., and Litman, B. J. (1990) *Biochemistry* **29,** 9135–9142
20. Niu, S. L., Mitchell, D. C., and Litman, B. J. (2001) *J. Biol. Chem.* **276,** 42807–42811
21. Mitchell, D. C., and Litman, B. J. (1998) *Biophys. J.* **74,** 879–891
22. Mitchell, D. C., Niu, S. L., and Litman, B. J. (2001) *J. Biol. Chem.* **276,** 42801–42806
23. Huster, D., Arnold, K., and Gawrisch, K. (1998) *Biochemistry* **37,** 17299–17308
24. Koenig, B. W., Strey, H. H., and Gawrisch, K. (1997) *Biophys. J.* **73,** 1954–1966
25. Niu, S. L., Mitchell, D. C., and Litman, B. J. (2002) *J. Biol. Chem.* **277,** 20139–20145
26. Leskov, I. B., Klenchin, V. A., Handy, J. W., Whitlock, G. G., Govardovskii, V. I., Bownds, M. D., Lamb, T. D., Pugh, E. N., Jr., and Arshavsky, V. Y. (2000) *Neuron* **27,** 525–537
27. Birch, D. G., Birch, E. E., Hoffman, D. R., and Uauy, R. D. (1992) *Investig. Ophthalmol. Vis. Sci.* **33,** 2365–2376
28. Eldho, N. V., Feller, S. E., Tristram-Nagle, S., Polozov, I. V., and Gawrisch, K. (2003) *J. Am. Chem. Soc.* **125,** 6409–6421
29. Birch, E. E., Birch, D. G., Hoffman, D. R., and Uauy, R. (1992) *Investig. Ophthalmol. Vis. Sci.* **33,** 3242–3253
30. Carlson, S. E., Ford, A. J., Werkman, S. H., Peeples, J. M., and Koo, W. W. (1996) *Pediatr. Res.* **39,** 882–888
31. Neuringer, M., Anderson, G. J., and Connor, W. E. (1988) *Annu. Rev. Nutr.* **8,** 517–541
32. Makrides, M., Simmer, K., Goggin, M., and Gibson, R. A. (1993) *Pediatr. Res.* **33,** 425–427
33. Lamptey, M. S., and Walker, B. L. (1976) *J. Nutr.* **106,** 86–93
34. Mills, D. E., Ward, R. P., and Young, C. (1988) *Nutr. Rev.* **8,** 273–286
35. Yamamoto, N., Okaniwa, Y., Mori, S., Nomura, M., and Okuyama, H. (1991) *J. Gerontol.* **46,** B17–B22
36. Bourre, J. M., Francois, M., Youyou, A., Dumont, O., Piciotti, M., Pascal, G., and Durand, G. (1989) *J. Nutr.* **119,** 1880–1892
37. Frances, H., Coudereau, J. P., Sandouk, P., Clement, M., Monier, C., and Bourre, J. M. (1996) *Eur. J. Pharmacol.* **298,** 217–225
38. Wainwright, P. E., Xing, H. C., Girard, T., Parker, L., and Ward, R. P. (1998) *Nutr. Neurosci.* **1,** 281–293
39. Greiner, R. S., Moriguchi, T., Slotnick, B. M., Hutton, A., and Salem, N. (2001) *Physiol. Behav.* **72,** 379–385
40. Catalan, J. N., Moriguchi, T., Slotnick, B., Greiner, R. S., and Salem, N., Jr. (2002) *Behav. Neurosci.* **116,** 1022–1031
41. Champoux, M., Hibbeln, J. R., Shannon, C., Majchrzak, S., Suomi, S. J., Salem, N., Jr., and Higley, J. D. (2002) *Pediatr. Res.* **51,** 273–281
42. Werkman, S. H., and Carlson, S. E. (1996) *Lipids* **31,** 91–97
43. Agostoni, C., Trojan, S., Bellu, R., Riva, E., and Giovannini, M. (1995) *Pediatr. Res.* **38,** 262–266
44. Birch, E. E., Garfield, S., Hoffman, D. R., Uauy, R., and Birch, D. G. (2000) *Dev. Med. Child Neurol.* **42,** 174–181